LIS1 RNA interference blocks neural stem cell division, morphogenesis, and motility at multiple stages

Jin-Wu Tsai,[1] Yu Chen,[1] Arnold R. Kriegstein,[2,3] and Richard B. Vallee[1,3]

[1]Department of Pathology and Cell Biology, [2]Department of Neurology, and [3]Center for Neurobiology and Behavior, College of Physicians and Surgeons, Columbia University, New York, NY 10032

Mutations in the human LIS1 gene cause the smooth brain disease classical lissencephaly. To understand the underlying mechanisms, we conducted in situ live cell imaging analysis of LIS1 function throughout the entire radial migration pathway. In utero electroporation of LIS1 small interference RNA and short hairpin dominant negative LIS1 and dynactin cDNAs caused a dramatic accumulation of multipolar progenitor cells within the subventricular zone of embryonic rat brains. This effect resulted from a complete failure in progression from the multipolar to the migratory bipolar state, as revealed by time-lapse analysis of brain slices. Surprisingly, interkinetic nuclear oscillations in the radial glial progenitors were also abolished, as were cell divisions at the ventricular surface. Those few bipolar cells that reached the intermediate zone also exhibited a complete block in somal translocation, although, remarkably, process extension persisted. Finally, axonal growth also ceased. These results identify multiple distinct and novel roles for LIS1 in nucleokinesis and process dynamics and suggest that nuclear position controls neural progenitor cell division.

Introduction

The human developmental disease classical lissencephaly is characterized by a nearly complete absence of gyri, an abnormally thickened four-layered cortex, and enlarged ventricles (Dobyns and Truwit, 1995). Classical, or type I, lissencephaly results from sporadic mutations in the LIS1 gene, resulting in LIS1 haploinsufficiency (Reiner et al., 1993; Lo Nigro et al., 1997). LIS1 was initially identified as a noncatalytic subunit of platelet-activating factor acetylhydrolase Ib (Hattori et al., 1994). Deletion of the catalytic subunits of platelet-activating factor acetylhydrolase, however, affects testicular rather than brain development (Koizumi et al., 2003; Yan et al., 2003). LIS1 orthologues have also been identified in the cytoplasmic dynein pathway in lower eukaryotes (Xiang et al., 1995), and biochemical and molecular studies have shown that LIS1 interacts with cytoplasmic dynein and its regulatory complex dynactin (Faulkner et al., 2000; Sasaki et al., 2000; Smith et al., 2000). LIS1 also interacts with other proteins initially identified in the dynein pathway: NudC (Morris et al., 1998), NudE (Efimov and Morris, 2000; Kitagawa et al., 2000), and its isoform NudEL (Niethammer et al., 2000).

Correspondence to Richard B. Vallee: rv2025@columbia.edu

A.R. Kriegstein's present address is Program in Developmental and Stem Cell Biology, University of California, San Francisco, San Francisco, CA 94143.

Abbreviations used in this paper: CP, cortical plate; IZ, intermediate zone; RNAi, RNA interference; shRNA, short hairpin RNA; siRNA, small interference RNA; SVZ, subventricular zone; VZ, ventricular zone.

The online version of this article contains supplemental material.

LIS1 orthologues are essential for nuclear migration and nuclear orientation in fungi (Xiang et al., 1995; Geiser et al., 1997). In dividing vertebrate cultured cells, LIS1 associates with kinetochores and the cell cortex (Faulkner et al., 2000). LIS1 also associates with centrosomes (Smith et al., 2000; Tanaka et al., 2004) and is located at the leading edge of migrating fibroblasts (Dujardin et al., 2003). Interference with LIS1 produces severe mitotic defects (Faulkner et al., 2000; Tai et al., 2002) and inhibits the redistribution of cerebellar granule cell soma within reaggregate cultures (Hirotsune et al., 1998) as well as the directed migration of fibroblasts (Dujardin et al., 2003; Kholmanskikh et al., 2003). How these cellular defects may contribute to the neuronal migration disorder and the agyric or pachygyric morphology of the lissencephalic brain is not completely understood.

Developmental analysis of LIS1 heterozygous mouse lines and of cells transfected with cDNA constructs for LIS1 RNA interference (RNAi) has shown abnormalities in the extent of neuronal redistribution (Hirotsune et al., 1998; Gambello et al., 2003; Shu et al., 2004). However, detailed analysis of the migration pathway has not been performed. Recent work on normal brain has indicated that this pathway is quite complex. Cortical neurons are generated directly from radial glial cells in the ventricular zone (VZ) or indirectly from intermediate progenitor cells in the subventricular zone (SVZ) that are themselves generated from radial glia (Noctor et al., 2001, 2004;

The Journal of Cell Biology, Vol. 170, No. 6, September 12, 2005 935–945
http://www.jcb.org/cgi/doi/10.1083/jcb.200505166

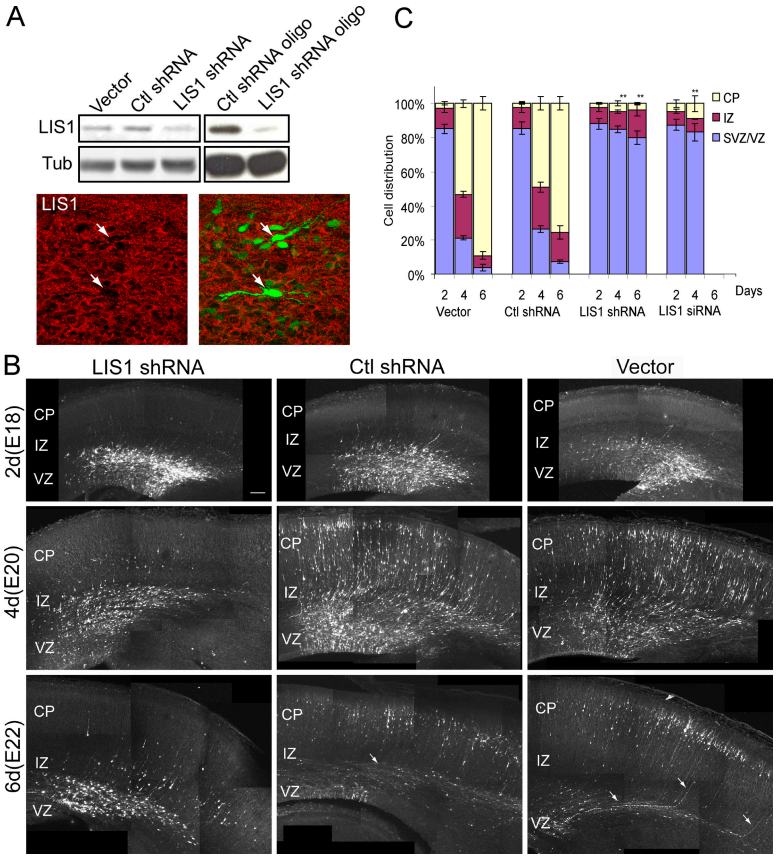

Figure 1. **Effect of RNAi on LIS1 expression and neural progenitor cell distribution.** (A, top) Western blot of LIS1 and tubulin in COS7 cells 48 h after transfection with LIS1 shRNA vectors or oligonucleotides. LIS1 levels in cells transfected with LIS1 shRNA or oligonucleotides were much lower than those in cells transfected with triple point mutated shRNA, empty vector, or control oligonucleotide. (Bottom) Immunostaining of LIS1 (red) in E18 rat neocortical neural progenitor cells transfected in utero at E16 with LIS1 shRNA vector, which also expresses GFP marker (green). Note the loss of LIS1 in GFP-expressing cells (arrows). (B) Disruption of cell redistribution in the neocortex by LIS1 RNAi. Coronal sections of rat brain 2, 4, and 6 d after electroporation at E16 with LIS1 shRNA, control shRNA, or empty vector. Cells expressing LIS1 shRNA were largely restricted to the VZ/SVZ, although some appeared within the lower IZ by days 4 and 6 (left). In contrast, cells transfected with control shRNA or empty vector migrated radially from the VZ to the CP with increasing time (middle and right). Note the additional lateral spread of VZ/SVZ cells in the control. Arrows, axonlike processes extending from migratory bipolar cells (see Altered Axonal Extension). Bar, 100 μm. (C) Percentages of cells transfected with empty, control shRNA, LIS1 shRNA vectors, and LIS1 siRNA oligonucleotide in different regions of the neocortex. The signal of Cy3-siRNA–transfected cells at day 6 was too low to detect. Error bars represent SEM. *t* test: *, $P < 0.05$; **, $P < 0.01$.

Haubensak et al., 2004). Neural progenitor cells are now known to progress through a series of morphogenetic stages. After classic interkinetic nuclear oscillations and cell division at the ventricular surface, newborn neurons ascend to the SVZ, where they convert to a multipolar nonmigratory phase (Rakic et al., 1974; Tabata and Nakajima, 2003; Noctor et al., 2004). After about a day, during which they begin to extend axonal processes, they convert to a bipolar stage and resume glial-directed radial migration. The importance of this complex progression in cortical development, how it is regulated, and how defects in this pathway may contribute to developmental diseases such as lissencephaly is not yet well understood.

This study was undertaken to gain insight into the specific role of LIS1 in neural progenitor behavior and neuronal cell migration. We conducted the first in situ live cell imaging analysis of neural progenitor cells with reduced LIS1 expression, and we followed the behavior of these cells throughout the migratory pathway. Surprisingly, migration and morphogenesis were blocked at multiple distinct stages, each of which has important implications for the biological function of LIS1 and for the physiological mechanisms underlying normal neurogenesis.

Results

Altered distribution of neuronal cells resulting from LIS1 inhibition

Studies of mouse strains that are heterozygous for LIS1 have revealed a human lissencephaly-like brain disorganization phenotype (Hirotsune et al., 1998; Cahana et al., 2001; Gambello et al., 2003). To allow us to explore a more complete range of LIS1 defects, to do so in a wild-type background, and to reveal cell-autonomous effects, we used RNAi and dominant negative cDNAs. For RNAi, we used both synthetic Cy3-labeled oligonucleotides and cDNAs based on the pRNAT-U6.1/Neo vector, which encodes a short hairpin RNA (shRNA) and coral GFP. The shRNA and small interference RNA (siRNA) sequences correspond to two different regions within LIS1, which are each conserved among multiple vertebrate species. To test the effectiveness of the shRNA construct and siRNA oligonucleotide on LIS1 expression, we transfected them into COS7 cells, which were lysed after 48 h and immunoblotted using anti-LIS1 antibody (Fig. 1 A, top). Most of the LIS1 protein was absent compared with control cells that were transfected with triple point mutant shRNA, empty vector, or scrambled siRNA oligonucleotide, respectively. We also stained brain sections with anti-LIS1 antibody 2 d after in utero electroporation with LIS1 shRNA vector and found the LIS1 signal to be absent in transfected cells (Fig. 1 A, bottom).

To examine the effects of LIS1 RNAi on brain development, LIS1 shRNA, control shRNA constructs, or empty vector were introduced into neural progenitor cells in rat neocortex by in utero electroporation at embryonic day (E) 16. GFP-positive cells in the VZ/SVZ, intermediate zone (IZ), or cortical plate (CP) were examined 2, 4, and 6 d later (Fig. 1, B and C; and Table S1, available at http://www.jcb.org/cgi/content/full/jcb.200505166/DC1). At day 2, cells that were transfected

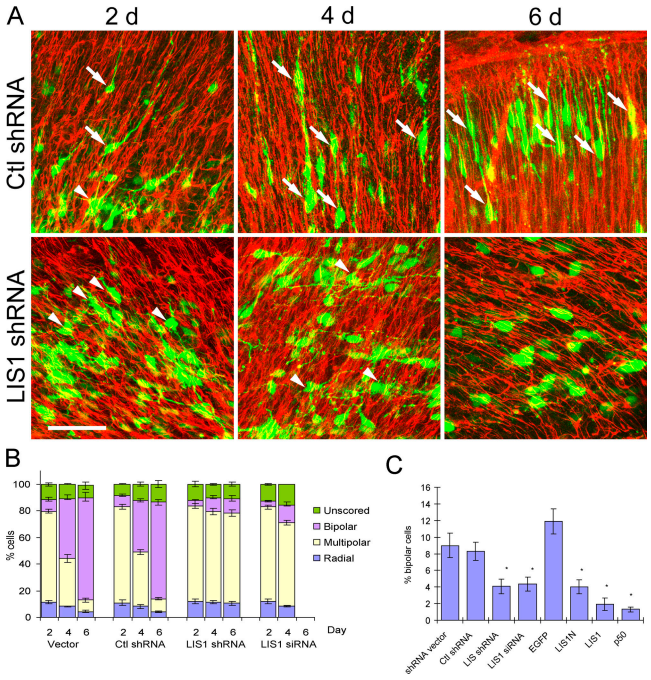

Figure 2. **Morphology of LIS1 shRNA–transfected cells.** (A) Morphology of cells transfected with control (top) and LIS1 shRNA (bottom) vectors (green) 2, 4, and 6 d after electroporation at E16 and counterstained with anti-nestin antibody (red). Many control cells migrated to the IZ and CP, where they became bipolar (arrows), whereas most LIS1 shRNA–transfected cells remained in the SVZ with a multipolar morphology (arrowheads). Bar, 50 μm. (B) Quantitative effects of LIS1 RNAi on cell morphology. In control brains, GFP-expressing radial glial and multipolar cells were maximal at posttransfection day 2 and decreased with time, and the number of bipolar cells increased. In LIS1 shRNA– and siRNA-transfected brains, the numbers of radial glial and multipolar cells remained relatively constant with time. (C) Comparison of bipolar cell number under diverse inhibitory conditions 2 d after electroporation. All dominant negative and siRNA constructs markedly decreased the ratio of bipolar to total transfected cells. Error bars represent SEM. *t* test: *, $P < 0.05$.

with LIS1 shRNA, control shRNA, and empty vector were largely found in the VZ and SVZ (88.2 ± 3.1%, $n = 4$ embryos; 86.5 ± 3.7%, $n = 3$ embryos; and 85.2 ± 2.9%, $n = 4$ embryos; respectively) with no obvious differences in spatial distribution between LIS1 shRNA– and control shRNA–transfected brains. By day 4, about half of GFP-positive control cells (control shRNA: 48.7 ± 3.9%, $n = 3$ embryos; empty vector: 53.1 ± 2.2%, $n = 5$ embryos) had become redistributed to the CP. By day 6, the majority of control cells had migrated to the CP (control shRNA: 75.3 ± 4.0%, $n = 3$ embryos; empty vector: 89.0 ± 3.9%, $n = 3$ embryos). The time course of redistribution in control neurons is consistent with previous observations in cells that were labeled with GFP that by using retroviral infection (Noctor et al., 2004) or in utero electroporation (Table S1).

In brains that were transfected with the LIS1 shRNA construct, however, the majority of transfected cells were still distributed in the VZ/SVZ at day 4 (84.9 ± 2.0%, $n = 5$ embryos), with only a subset having reached the lower region of the IZ (10.4 ± 0.8%, $n = 5$ embryos). By day 6, cells expressing LIS1 shRNA had an almost identical distribution to that observed at days 2 and 4 (80.1 ± 4.0% in VZ/SVZ; 16.2 ± 3.3% in IZ; $n = 3$ embryos). Thus, the knockdown of LIS1 by RNAi in neurons appeared to have a direct effect on radial redistribution to the CP. A virtually identical migration arrest was produced by LIS1 siRNA oligonucleotide at days 2 and 4 (Fig. 1 C). However, the signal of the fluorescent siRNA oligonucleotide was too weak to detect by day 6, probably as a result of degradation or dilution of the fluorochrome or RNA. We note that the redistribution of LIS1 shRNA–expressing cells was inhibited not only at the center of the neocortex but also at its lateral boundaries. In these regions, the radial glial fibers are themselves distorted (Fig. S1, available at http://www.jcb.org/cgi/content/full/jcb.200505166/DC1; Misson et al., 1991), and migration along these tracks likely contributes to cortical expansion.

We also introduced full-length LIS1 (GFP-LIS1), an NH_2-terminal LIS1 fragment (GFP-LIS1N), and the full-length dynamitin subunit of the dynactin complex (GFP-p50), each of which produce dominant inhibitory effects on dynein function in cultured cells (Echeverri et al., 1996; Faulkner et al., 2000; Tai et al., 2002). No clear effect on overall cell distribution was observed 2 d after the expression of each of these constructs, but a marked decrease in transfected cell number was observed by day 4. These results suggest that prolonged overexpression of these cDNA constructs may be lethal.

Accumulation of LIS1 and dynactin inhibited cells at the multipolar stage

As noted previously, newborn neurons have been shown to move from the VZ to the SVZ and assume an immobile multipolar morphology before converting to a bipolar morphology and recommencing their radial migration (Tabata and Nakajima, 2003; Noctor et al., 2004). To investigate the involvement of LIS1 in the specific stages in this pathway, we performed morphological analysis of the transfected cells. Individual radial glial, multipolar, and bipolar cells in different regions were readily distinguishable from the analysis of serial confocal images of brain slices (Fig. 2 A). In control brains, many multipolar cells were produced by day 2, constituting a majority of the population in the SVZ (control shRNA: 72.2 ± 1.7%, $n = 4$ embryos; empty vector: 68.3 ± 1.5%, $n = 3$ embryos; Fig. 2 B). Some cells in the lower SVZ and VZ still showed a radial glial morphology (control shRNA: 10.9 ± 2.1%, $n = 4$ embryos; empty vector: 11.4 ± 1.0%, $n = 3$ embryos). Some cells in the upper SVZ and a few cells that had reached the IZ exhibited prominent leading processes extending toward the CP (Fig. 2 A) as expected for bipolar migratory neurons (control shRNA: 9.0 ± 1.4%, $n = 5$; empty vector: 8.3 ± 1.1%, $n = 3$; Fig. 2 B). By days 4 and 6, the numbers of cells with radial glial and multipolar morphology were decreased, the majority of control cells had become bipolar (control shRNA: 38.6 ± 1.4%, $n = 3$ embryos and 72.6 ± 1.8%, $n = 3$ embryos; empty vector: 44.6 ± 3.3%, $n = 5$ embryos and 76.8 ± 3.9%, $n = 3$ embryos, respectively; Fig. 2 B), and many had migrated to the CP.

In LIS1 shRNA–transfected brains, multipolar cells again constituted the majority of the cell population by day 2 (71.6 ± 1.8%, $n = 4$ embryos) as they did in control brains. At days 4

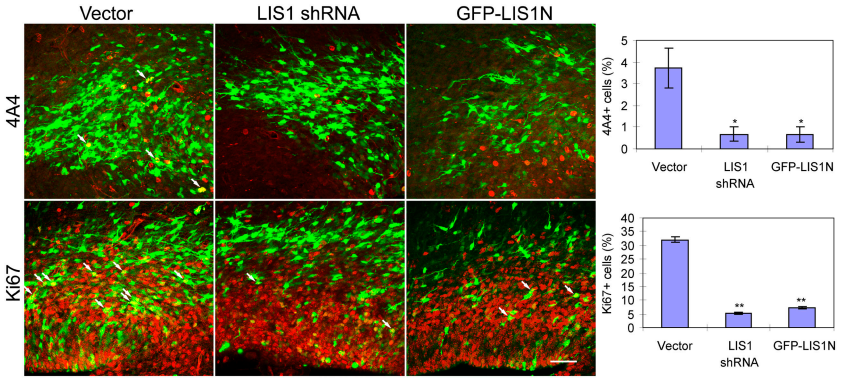

Figure 3. **Cell cycle stage of transfected cells.** Brains were transfected with empty vector, LIS1 shRNA, or GFP-LIS1N (green) at E16 and, 2 d later, were immunostained with antibodies to the M-phase marker phosphovimentin (4A4, red; top), and Ki67 (red; bottom), which is a transcription factor expressed from S through M phase. Transfected cells positive for either marker appear yellow (arrows). Bar, 50 μm. The percentage of total transfected cells that were positive for 4A4 or Ki67 was reduced significantly in LIS1 shRNA– and GFP-LIS1N–transfected brains relative to controls. Error bars represent SEM. *t* test: *, $P < 0.05$; **, $P < 0.01$.

and 6, however, most of the cells were not only stalled in the SVZ (Fig. 2 A) but, strikingly, were mostly multipolar (68.0 ± 2.5%, $n = 5$ embryos; and 67.7 ± 2.6%, $n = 3$ embryos, respectively; Fig. 2 B). Only a limited number of bipolar cells were present in the lower IZ at days 2–6 (4.1 ± 0.9%, $n = 4$ embryos; 10.3 ± 1.5%, $n = 5$ embryos; and 10.6 ± 2.3%, $n = 3$ embryos at days 2, 4, and 6, respectively), and limited numbers of cells with radial morphology also persisted throughout (12.0 ± 1.6%, $n = 4$ embryos; 11.4 ± 1.0%, $n = 5$ embryos; and 10.7 ± 1.4%, $n = 3$ embryos at days 2, 4, and 6, respectively). A similar accumulation of cells with a multipolar morphology was observed on days 2 and 4 in brains that were transfected with Cy3-LIS1 siRNA oligonucleotides (Fig. 2 B and Fig. S2, available at http://www.jcb.org/cgi/content/full/jcb.200505166/DC1). Although cells overexpressing dominant negative cDNA constructs could only be monitored through day 2, a decrease in the percentage of bipolar cells was also observed (GFP control: 11.9 ± 1.5%, $n = 3$; GFP-LIS1N: 4.0 ± 0.8%, $n = 3$; and GFP-LIS1: 2.0 ± 0.8%, $n = 2$; Fig. 2 C and Fig. S2). Together, these results suggested that accumulation in the SVZ reflected a block in exit from the multipolar stage of the migratory pathway.

To evaluate the differentiation state of SVZ cells, sections were stained with the neuronal marker TuJ1 (Fig. S3, available at http://www.jcb.org/cgi/content/full/jcb.200505166/DC1) and progenitor cell markers nestin (Fig. 2 A) and vimentin (not depicted). Multipolar and bipolar cells that were transfected with LIS1 shRNA, siRNA oligonucleotides, GFP-LIS1N, GFP-LIS1, or GFP-p50 all expressed the neuronal marker TuJ1 but not nestin and vimentin, as is the case for cells transfected with control plasmids or infected with retrovirus (Noctor et al., 2004). These results provided further support that cells with reduced LIS1 expression were arrested in a stage corresponding to the multipolar stage of postmitotic neurons in normal brain.

LIS1 has been implicated in cell division by its localization to mitotic kinetochores and the mitotic cell cortex of nonneuronal cells. Dominant negative cDNAs, antibody microinjection, and antisense oligonucleotides all resulted in a pronounced accumulation of cells in prometaphase (Faulkner et al., 2000; Tai et al., 2002). To test for changes in neural progenitor cell cycle progression, brains that were transfected with the empty vector, LIS1 shRNA, or GFP-LIS1N constructs were stained on day 2 using the antiphosphovimentin antibody 4A4, which labels M-phase neural progenitor cells. In control brains that were transfected with empty vector, 3.7 ± 0.9% ($n = 4$) of GFP-expressing cells in the VZ/SVZ were 4A4 positive (Fig. 3, top). To our surprise, very few LIS1 shRNA– and GFP-LIS1N–transfected cells were 4A4 positive (0.68 ± 0.33%, $n = 4$; and 0.67 ± 0.35%, $n = 3$; respectively). We also immunostained cells for the nuclear transcription factor Ki67, which is expressed in proliferating cells from S-phase through M-phase of the cell cycle. In day 2 control cells, which were primarily located within the VZ/SVZ, 32.0 ± 4.3% ($n = 4$) of the cells were Ki67 positive (Fig. 3, bottom). In contrast, the percentages of Ki67-positive cells in LIS1 shRNA– (5.4 ± 1.2%, $n = 4$) and GFP-LIS1N (7.2 ± 1.5%, $n = 3$)–transfected brains were dramatically decreased ($P < 0.01$).

Block in multipolar to bipolar conversion in the SVZ

The mechanisms underlying the conversion of nonmigratory multipolar cells in the SVZ to the bipolar migratory state have not been explored. The accumulation of LIS1-inhibited cells in the multipolar state suggested an important role for LIS1 in this process. To test this possibility directly, slices from brain tissue that had been transfected with LIS1 or control shRNA constructs were placed in culture for live cell imaging. By using a 10-min time-lapse interval during a 10–18-h period from day 2, we detected 14 examples of this morphogenetic event among 73 multipolar cells from 3 brain slices that were examined (Fig. 4; Videos 1 and 2, available at http://www.jcb.org/cgi/content/full/jcb.200505166/DC1). Initially, the cells had multiple processes extending and retracting actively, at which time the cell body appeared relatively immobile. Just before the morphological conversion event, one of the preexisting processes increased in girth and became the leading migratory process as other processes retracted. The newly emergent migratory processes tended to orient toward the pial surface, suggesting an interaction with radial glial fibers, as shown in fixed brain tissues that were stained with nestin and vimentin (Fig. S1). Finally, the cell body followed the direction of the leading process and migrated away. Altogether, the conversion event took only 61 ± 5 min ($n = 14$ cells) to complete.

Almost all of the cells that were transfected with the LIS1 shRNA construct were multipolar and possessed an overall appearance that is similar to that of multipolar control cells (Fig. 4

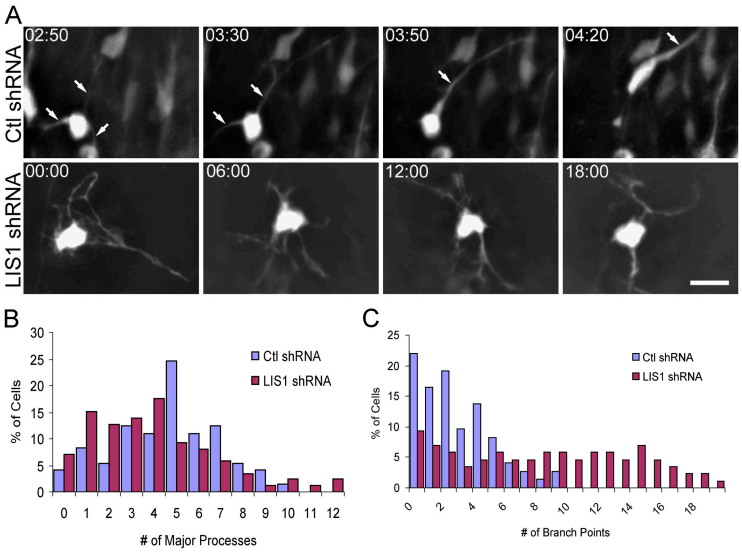

Figure 4. **Live cell imaging of the conversion of neural progenitor cells from multipolar to bipolar morphology.** (A) Slices from rat brain electroporated in utero with control or LIS1 shRNA vector at E16 were placed into culture at E18 and imaged every 10 min by GFP fluorescence microscopy. Multiple processes of the control neuron at the top (arrows) give way to a single major process at the top as the cell initiates radial migration (Videos 1 and 2, available at http://www.jcb.org/cgi/content/full/jcb.200505166/DC1). Cell expressing shRNA for LIS1 (bottom) persisted in the multipolar state for 18 h of observation (Video 3). Time is shown in hours/minutes. Bar, 10 μm. (B) Number of primary processes emanating from a multipolar cell body varied over a broad but similar range in control versus LIS1 shRNA–transfected cells. (C) Number of process branch points per cell were increased in LIS1 siRNA–transfected cells versus controls.

A and Video 3, available at http://www.jcb.org/cgi/content/full/jcb.200505166/DC1). The most dramatic difference was that the transition from the multipolar to the migratory state was completely abolished (0/86 cells in 4 slices), directly demonstrating a block in the migratory pathway at a highly specific stage. In several other regards, experimental and control cells were fairly similar. The number of primary processes (directly protruding from the cell body) was comparable between LIS1 shRNA–transfected cells (3.9 ± 0.3, n = 86 cells) and control cells (4.7 ± 0.3, n = 73 cells; Fig. 4 B), and the lifetime (119 ± 4 min, n = 343 processes) was similar to that of the primary processes of control cells (124 ± 3 min, n = 336 processes), indicating that the stability of primary processes was not affected by LIS1 RNAi. However, despite the similarity in overall cell shape, significant differences could be observed. The primary processes in LIS1 shRNA–transfected cells were more branched (8.3 ± 0.7 branch points/cell, n = 73 cells) than in control cells (2.6 ± 0.3 branch points/cell, n = 86 cells; Fig. 4 C). The branches were usually short (3.5 ± 0.1 μm, n = 711 branches) and, more dramatically, as observed in time-lapse video (Video 3), were far less stable than the primary processes, with an average lifetime of 26 ± 1 min (n = 711 branches).

Finally, we examined videos of control and shRNA-transfected cells for the frequency of mitotic events. Consistent with our immunohistochemical analysis, we observed that 8/73 control cells divided during time-lapse periods of 12–18 h (Video 4, available at http://www.jcb.org/cgi/content/full/jcb.200505166/DC1). In contrast, 0/86 LIS1 shRNA–transfected cells were observed to divide during a comparable period.

Block in interkinetic nuclear oscillations and cell division in radial glial cells

Despite the accumulation of multipolar cells in the SVZ, we still found that a small percentage of radial glial cells remained in the VZ of LIS1 shRNA–transfected brains (Figs. 1 B and 2 B). To test whether these cells were still motile, live cell imaging of brain slices was again performed. In control shRNA–transfected cells, nuclei were observed to oscillate, albeit in a discontinuous fashion: periods of immobility were followed by relatively rapid directed movements toward (n = 13/28) or away (n = 11/28) from the ventricular surface (Fig. 5 A and Video 5, available at http://www.jcb.org/cgi/content/full/jcb.200505166/DC1). LIS1 shRNA–transfected radial glial cells appeared to be morphologically normal, exhibiting their characteristic long bipolar radial processes. Surprisingly, however, nuclear movement was almost completely abolished among all of the 23 cells from 3 embryos that were monitored. Random movements of very limited range (1–5 μm) were still observed, but directed nuclear migration over substantial distances was eliminated (Fig. 5 B and Video 6, available at http://www.jcb.org/cgi/content/full/jcb.200505166/DC1). Nuclei were stalled at various distances from the ventricular surface and maintained their positions over substantial periods of time.

Nuclear division is well established to correlate with position relative to the ventricular surface, although the functional basis for this relationship remains an important mystery in brain development. Among 28 control radial glial cells, 9 were observed to divide during 10–15 h each of direct observation. All divisions occurred at the ventricular surface. In marked contrast, no cell divisions were detected in LIS1 shRNA–transfected radial glial cells (n = 0/23 cells in three slices), nor were cells arrested with condensed chromosomes (unpublished data). These results suggest that migration of the nucleus to the ventricular surface is required for radial glial cell division.

Impaired radial migration of bipolar cells

Our results identified two distinct forms of neural progenitor cell behavior that were completely inhibited by LIS1 RNAi. Nonetheless, some cells with a bipolar morphology reached the lower IZ (Fig. 1 B). To test whether these cells represented a motile subpopulation of LIS1 shRNA transfectants, live cell imaging was again performed. In control brains, migrating bipolar cells in the IZ were observed between days 3 and 4. The cells extended a leading process toward the CP of relatively constant length (Fig. 6 A, top; and Video 7, available at http://www.jcb.org/cgi/content/full/jcb.200505166/DC1). Movement

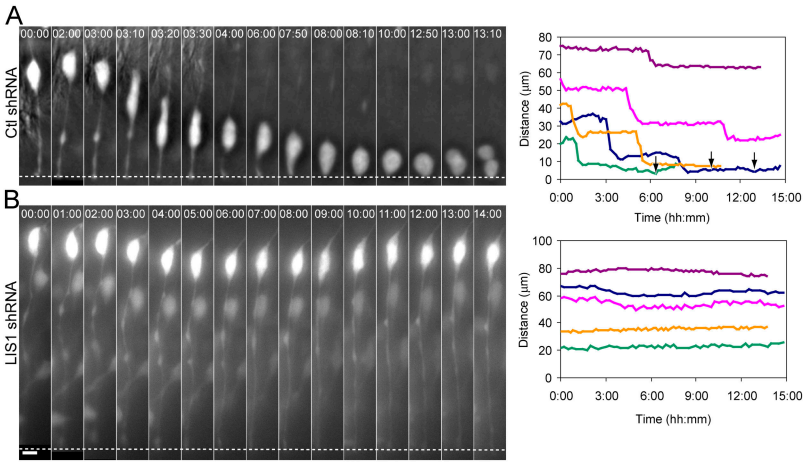

Figure 5. **Live cell imaging of neural progenitor cell behavior within the VZ.** (A) Cell body of a control progenitor cell at the radial glial stage migrates away from and then toward the ventricular surface (dotted lines), where it divides by the last time point (Video 5, available at http://www.jcb.org/cgi/content/full/jcb.200505166/DC1). Tracings of cell body positions for five typical controls show rapid but discontinuous movements. Arrows indicate the time of cell division. (B) Cell body of a LIS1 shRNA–transfected cell is relatively immobile over a 14-h time period (Video 6). Tracings show that the cell body position is relatively constant and that stepwise changes are not observed. Note that the behavior of cell bodies in control and experimental cases are independent of starting position relative to the ventricular surface. Times are shown in hours/minutes. Bar, 5 μm.

of the cell bodies was discontinuous as the cell underwent locomotion toward the pial surface.

In LIS1 shRNA–transfected tissue, there were fewer labeled cells (as noted previously) in the IZ (Table S2, available at http://www.jcb.org/cgi/content/full/jcb.200505166/DC1). The limited number of cells that reached the IZ still had an overall bipolar morphology. However, the soma of all monitored cells from two embryos were completely immobile (Fig. 6 A, bottom; and Video 8, available at http://www.jcb.org/cgi/content/full/jcb.200505166/DC1). Despite this pronounced inhibitory effect, the leading processes still exhibited active motility. Numerous short and short-lived branches (8.7 ± 1.6 branches/cell, $n = 7$ cells) were observed versus control bipolar cells (1.7 ± 0.2 branches/cell, $n = 26$ cells; Fig. 6 B). More remarkably, process length increased with time (growth rate = 0.95 ± 0.12 μm/min, $n = 7$ cells; Fig. 6 C). In control cells, the leading process and soma moved at similar rates (0.85 ± 0.07 and 0.83 ± 0.07 μm, $n = 26$ cells; Fig. 6 C), and, hence, the length of the leading process remained relatively constant (47.6 ± 5.8 μm, $n = 26$ cells; in all cases, cells were recorded before the leading process reached the pial surface). A striking net result was that the leading tip of experimental and control processes extended at almost identical rates (Fig. 6 C). We did not observe branched migration in these cells, as has been reported in studies of p35 mutant (Gupta et al., 2003) and wild-type mice (Tabata and Nakajima, 2003).

Altered axonal extension

In developing neocortex, most migrating neurons put out a trailing process (Fig. 1 B, arrows), which is thought to represent the developing axon (Schwartz and Goldman-Rakic, 1991; Noctor et al., 2004). These processes persist as the cells become bipolar and move toward the CP. Despite the accumulation of LIS1 shRNA–transfected cells in the SVZ, tangential axonlike processes were observed at days 4 and 6 (Fig. 7, A and B). These processes extended medially in the same direction as seen for control cells. However, the axonlike processes in LIS1 shRNA–transfected cells were shorter and somewhat curved and branched (Fig. 7 A). The role of LIS1 in this aspect of neural progenitor behavior has not been previously studied. For this reason and to gain further support for the origin and character of these processes, we monitored their behavior in living slices.

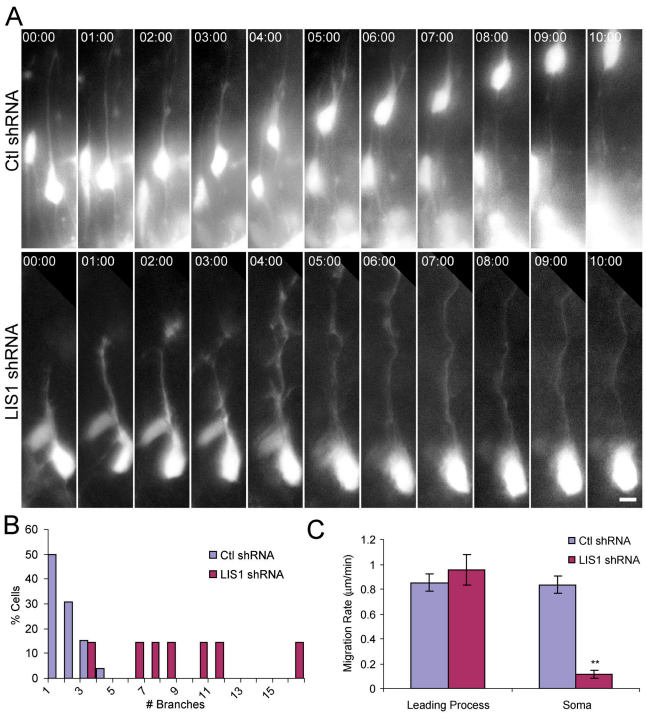

Figure 6. **Live cell imaging of neural progenitor cell behavior within the IZ.** Rat brains were electroporated with LIS1 (bottom) or control shRNA (top) constructs at E16, and the brains were sectioned and cultured 3 d later. (A) Images from bipolar cells within the IZ. Control cells extended a leading process toward the CP, and the cell body followed, resulting in forward locomotion with a process of relatively constant length (Video 7, available at http://www.jcb.org/cgi/content/full/jcb.200505166/DC1). When transfected with LIS1 shRNA, the leading process of the cells continued to grow, but the cell body remained immobile. The leading process also extended many short projections along its length (Video 8). Time is shown in hours/minutes. Bar, 5 μm. (B) Branching of leading process in the IZ. Control cells normally had one to three branches, whereas there were many small branches in LIS1 shRNA–transfected cells. (C) Rate of leading process extension and somal migration. The rate of process extension was almost unchanged by LIS1 RNAi, but somal movement was largely abolished. Error bars represent SEM. *t* test: **, $P < 0.01$.

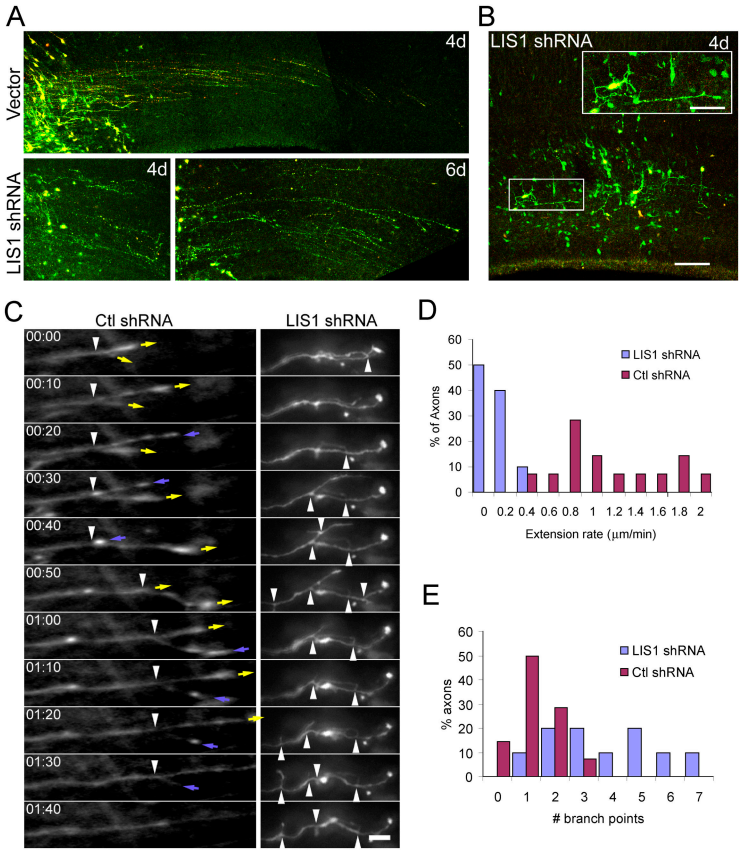

Figure 7. **Live cell imaging of axonlike processes.** Rat brain was electroporated with control or LIS1 RNAi construct at E16. (A) Fixed images of axonlike processes in control (vector) cells 4 d posttransfection (top). These processes extend tangentially toward the medial line from most postmitotic neurons in the SVZ and IZ. In LIS1 shRNA–transfected brains, axonlike processes were observed in the same orientation, although they were shorter, more curved, and more branched (bottom panels show days 4 and 6 posttransfection). (B) Most of the axonlike processes in LIS1 shRNA–transfected cells could be seen to originate from multipolar cells. Bar, 100 μm. Box shows the magnification of a multipolar cell extending an axonlike process. Bar, 20 μm. (C) Live cell imaging of axonal growth. Rat brain sections were placed into culture 2 d after electroporation, and images were recorded from the SVZ every 10 min. (Left) The control axons usually possessed only one branch point (arrowheads), with the two branches alternatively growing (yellow arrows) and retracting (blue arrows), resulting in an overall steady pattern of axonal elongation (0.7 μm/min in example shown; Video 9, available at http://www.jcb.org/cgi/content/full/jcb.200505166/DC1). (Right) Axons transfected with LIS1 shRNA construct exhibited multiple short branches (arrowheads indicate branch points), which extended and retracted dynamically. The overall length of the axon, however, stayed virtually constant (Video 10). Time is shown in hours/minutes. Bar, 10 μm. (D) Axonal growth rate. Axons of LIS1 shRNA–transfected cells grew much more slowly than controls. (E) Axonal branching was also substantially increased in LIS1 shRNA–transfected cells.

In control cells, these processes could be traced back to multipolar SVZ or bipolar IZ cells (Fig. 1 B) and could be observed to extend toward the medial side of the neocortex at a relatively constant rate of 1.19 ± 0.13 μm/min (n = 14 axons), which is consistent with their identification as axons (Fig. 7 C and Video 9, available at http://www.jcb.org/cgi/content/full/jcb.200505166/DC1). The axons typically had two terminal branches, which alternatively extended and retracted and were tipped by growth cone-like lamellar enlargements. In cells that were transfected with LIS1 shRNA, axons could still be distinguished among the multiple processes of SVZ cells (Fig. 7 C and Video 10, available at http://www.jcb.org/cgi/content/full/jcb.200505166/DC1). However, their rate of extension was greatly reduced (0.16 ± 0.04 μm/min; Fig. 7 D), although their orientation was close to that of normal cells. These processes tended to be more highly branched (3.8 ± 0.6 branch points/axon, n = 10 axons) than normal (1.3 ± 0.4 branch points/axon, n = 14 axons; Fig. 7 E). These branches were very dynamic and had a short average lifetime of 39 ± 4 min (n = 38 branches). Importantly, net forward extension of the axons was virtually eliminated.

Discussion

Using RNAi and overexpression of dominant negative constructs, we found that acute interference with LIS1 expression or function in a wild-type background dramatically inhibited the redistribution of neural progenitor cells during neocortical development. Our live imaging analysis of LIS1 knockdown cells provided direct evidence for virtually complete arrest at multiple steps of neurogenesis: (1) interkinetic nuclear oscillations within the radial glial cells and the attendant mitotic divisions; (2) conversion of multipolar SVZ cells to the bipolar migratory state; (3) the locomotion of bipolar cells through the IZ; and (4) the axonal growth of migratory neurons (Fig. 8). This pattern of effects is inconsistent with a single general effect on neural progenitor cell maturation or migration. It is more readily explained as the result of distinct effects at a number of different stages in the migratory and cell cycle pathways. We speculate that this outcome is a result of uptake of the shRNA-expressing vector at a range of concentrations and cell cycle stages by neural progenitor cells that are exposed at the ventricular surface. This pattern of inhibition appears to provide a unique means to gain direct insight into the complete range of neuronal functions in which LIS1 participates. Each of the observed effects, in turn, provides new insight into the etiology of lissencephaly.

LIS1 is essential for interkinetic nuclear oscillation and entry into cell division

The earliest aspect of neurogenesis in which LIS1 is implicated by our data are the interkinetic nuclear oscillations of neural progenitor cells within the VZ (Fig. 5), which have only recently been identified as radial glial cells (Malatesta et al., 2000; Miyata et al., 2001; Noctor et al., 2001). In control radial glial cells, somal movements were saltatory but mostly unidi-

rectional during the substantial periods of continuous observation that were involved in our experiments (Fig. 5). LIS1 RNAi completely abolished directed somal motility. This result represents the first direct demonstration that LIS1 is involved in the classic interkinetic nuclear oscillations of mammalian neural progenitor cells. It supports the hypothesis that vertebrate LIS1, like its fungal counterpart *NudF* (Xiang et al., 1995), is involved in nuclear translocation within cell processes. Thus, our results indicate that dynein, as regulated by LIS1, is the force generator for nuclear movement in radial glial progenitors.

A long-standing issue in the field of brain development is the functional significance of interkinetic nuclear oscillations: does nuclear position merely correlate with cell cycle stage or does it control it? We observed no mitotic events in cells expressing LIS1 shRNA, which is in dramatic support of the latter possibility. This evidence could relate to the defects in cell division resulting from the expression of dominant negative cDNAs, antibody injection, and antisense oligonucleotides in our previous work (Faulkner et al., 2000; Tai et al., 2002). However, each of these treatments caused cells to accumulate in prometaphase with a markedly increased mitotic index overall. This contrasts dramatically with the current situation in which no mitotic events were observed in VZ and SVZ progenitor cells, and mitotic index was substantially reduced. We argue, therefore, that the current observed decrease in mitotic cells must have a different cause.

In the case of radial glial cells in the VZ, an appealing possibility is that known or unknown mitogenic factors that are enriched at the ventricular surface are required not only in controlling neurogenesis but also in controlling mitotic entry. In this case, the inability of nuclei to reach the ventricular surface in our experiments would limit their access to mitogenic agents. This possibility is supported by a decrease in the percentage of LIS1 shRNA–transfected radial glial cells that are positive for phosphovimentin or that exhibit condensed chromosomes as judged by DAPI staining (unpublished data). Intriguingly, the few mitotic cells we did see in the latter analysis were all located at the ventricular surface. These may represent rare cells not yet detected by our live cell imaging, which retained sufficient LIS1 to enter mitosis. However, their exclusive location at the ventricular surface further supports a spatial control mechanism for mitotic entry.

We also observed a reduced number of mitotic figures within the SVZ in fixed brain tissue and in the number of Ki67-positive multipolar cells (Fig. 3). Thus, it appears that the number of SVZ intermediate progenitor cells, which are still capable of division (Noctor et al., 2004), was significantly reduced by interference with LIS1 expression or function. It is unclear whether the reduced numbers of mitotic cells that we observed within the VZ and SVZ result from related mechanisms. We suspect that those transfected cells that reach the SVZ cells must, nonetheless, have experienced some effect of reduced LIS1 expression (e.g., a slower journey to their final destination). Conceivably, such a delay could alter fate determination for these cells, allowing premature exit from the cell cycle.

In a previous study with an LIS1 heterozygote mouse, cell divisions were reported to increase in the SVZ but decrease

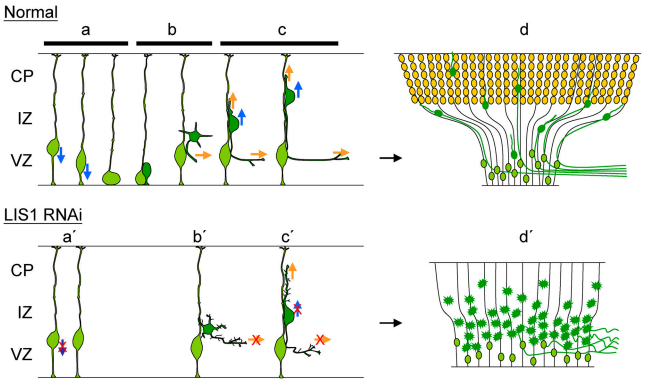

Figure 8. **Schematic diagram showing the effects of LIS1 inhibition on neural progenitor cell proliferation, migration, and morphogenesis.** (Top) Cortical neurons undergo distinct phases of neurogenesis and migration (Noctor et al., 2004). (a) The first step involves bidirectional interkinetic nuclear oscillations within radial glial cells (light green). Cell division occurs at the ventricular surface. (b) Postmitotic neurons (dark green) then migrate away from the ventricle and become paused in a multipolar state within the VZ/SVZ as they extend an axon. (c) Cells convert to a bipolar morphology and migrate along radial fibers to the CP as axonal growth continues. (d) As the orientation of radial fibers becomes distorted by cortical expansion, neuronal migration becomes increasingly outward directed. (Bottom) Neural progenitor cells exhibit as many as three discrete terminal effects of LIS1 RNAi. (a′) Radial glial cells cease interkinetic nuclear migration, and cell division is inhibited. (b′) Multipolar cells fail to transition to the bipolar migratory stage. (c′) Bipolar cells extend a leading process at normal rates, but the cell soma remains stationary. Although axons are extended from both multipolar and bipolar cells, the axons are more curved, branched, and grow more slowly. (d′) A preponderance of cells are arrested within the SVZ, resulting in subcortical band heterotopia, which is associated with classical lissencephaly. Both radial migration and lateral dispersion are disrupted, preventing neuronal cells from inserting into the CP and from contributing to further lateral spread. Blue and orange arrows indicate cell body movements and process extension, respectively. Red crosses indicate blocking of these activities.

in the VZ (Gambello et al., 2003). Although these divisions were said to be in part "ectopic," it was not possible to distinguish whether they involved radial glial or SVZ intermediate progenitor cells. These results, therefore, cannot be readily related to our study. However, based on our current and previous results, we predict that cell division should proceed under conditions of haploinsufficiency, albeit at a reduced frequency. Division itself, however, should be prolonged. The net result may have different effects on mitotic index in the VZ and SVZ, but the precise quantitative outcome is difficult to predict. We note that increased ectopic divisions were recently reported in mice that were heterozygous null for NudE, which is another protein in the LIS1 and dynein pathway (Feng and Walsh, 2004). Thus, as predicted from in vitro studies (Faulkner et al., 2000), brain developmental disorders arising from mutations in the dynein pathway now appear to involve defects in cell proliferation as well as in migration.

LIS1 is necessary for progression from the multipolar to the migratory stage

The most striking effect of LIS1 RNAi and dominant negative LIS1 and dynactin cDNAs on the overall distribution of transfected neural progenitors was the accumulation of cells within the SVZ (Fig. 2), as was previously observed in RNAi analysis

of the lissencephaly genes doublecortin (LoTurco, 2004) and LIS1 (Shu et al., 2004). Whether this pattern reflected a general migration delay or interference with specific steps in the migratory pathway was unknown. Our results demonstrate the latter to be the case. Although the previous study involving the use of LIS1 RNAi reported the bipolar morphology to be predominant in the SVZ (Shu et al., 2004), our evidence using both static and live cell imaging showed an absolute block in progression from the multipolar to the migratory stage (Fig. 4).

A specific block in exit from the SVZ is of considerable interest in understanding lissencephaly. This condition is characterized by the presence of a broad ectopic neuronal lamina within the white matter of the newborn neocortex (Dobyns and Truwit, 1995). Based on our results, we propose that this and, perhaps, other lamination defects reflect changes in specific rate-limiting steps in the neuronal migration pathway, predominantly involving exit from the SVZ.

The specific role of LIS1 in the conversion of multipolar to bipolar cells is uncertain. The first detectable event in this process was a thickening of the presumptive migratory process, which the nucleus subsequently enters (Fig. 4). This observation suggests that LIS1 and its regulatory target dynein are involved in the shift in cytoplasmic contents into the differentiating migratory process. We have previously observed that dynein and LIS1 are associated with the leading edge of migrating fibroblasts (Dujardin et al., 2003). More recently, we have observed a similar accumulation of dynein and LIS1 at the tips of rapidly growing laminin-induced neurites in primary chick dorsal root ganglia neurons (unpublished data). We suspect that LIS1 and dynein may be playing a related role in the initiation of the migratory process, although, not surprisingly, in its subsequent growth (see next section). Our results also suggest that at the reduced levels attained in this study, LIS1 is not required for entry into the multipolar state or in process maintenance. Whether the observed changes in process dynamics and morphology reflect the effects of residual LIS and whether further reduction in LIS1 would eliminate processes entirely remains to be seen.

Uncoupling of nucleokinesis from migratory process growth

The number of LIS1 siRNA–, shRNA-, and dominant negative LIS1- and dynactin cDNA–transfected cells within the IZ and CP were greatly reduced relative to controls, which is consistent with a small probability of escape from the SVZ (Fig. 1). Those few cells that reached this region were not yet connected with the pial surface of the developing brain. Migration should, therefore, occur by locomotion (Nadarajah et al., 2001), which involves forward extension of the migratory process and somal translocation to keep up. The shRNA-expressing cells had a bipolar morphology, which is comparable in low magnification images with control cells. However, migration was completely abolished.

In striking contrast to normal bipolar cells, however, the soma were virtually immotile (Fig. 6). Nonetheless, growth of the migratory process persisted. Together, these results provide the first indication that these aspects of locomotion can be uncoupled. As is the case for SVZ cells, the migratory processes of LIS1 shRNA–transfected IZ cells exhibited numerous short, highly dynamic extensions. Whether these represent branches that are similar to those observed in axons or whether they are more similar to filopodial extensions is unclear. Curiously, we found net axonal growth to stop in LIS1 knockdown cells, whereas the leading migratory processes of bipolar cells maintained their ability to extend. One possible explanation for these differences is that the migratory process, but not the axon, is guided and supported by radial glial fibers, where dynein and LIS1 might be less essential. In any case, our results indicated that the basic roles of dynein and LIS1 may differ between process types.

Other studies have found that reduced expression of LIS1 and its interacting proteins NudE and NudEL or dynein inhibited somal translocation in dissociated neuronal cell cultures (Hirotsune et al., 1998; Gambello et al., 2003; Shu et al., 2004; Tanaka et al., 2004). Clear effects on somal movement were observed, but it is uncertain whether they represent nuclear migration within processes or traction-mediated translocation of the entire somal region. Recent evidence has suggested a role for LIS1, dynein, and NudEL in generating tension between the nucleus and centrosome in migratory neural progenitor cells (Shu et al., 2004; Tanaka et al., 2004), which could contribute to somal translocation (Solecki et al., 2004). Based on evidence from other systems, this behavior is likely to be mediated by cortically associated dynein and LIS1, with which centrosome-tethered microtubules interact (Palazzo et al., 2001; Dujardin et al., 2003; Etienne-Manneville and Hall, 2001). We suspect that the observed defect in somal movement within bipolar IZ cells that were transfected with LIS1 shRNA may, in part, involve a similar pool of cortical dynein that is unable to engage cytoplasmic microtubules.

LIS1 is important in axonal extension

We could detect a single long axon extending from both multipolar and bipolar cells based on outgrowth length, caliber, and direction of the process. The axon remained clearly identifiable in cells that were subjected to LIS1 RNAi, demonstrating the persistence of underlying polarity in multipolar and bipolar cells. The persistence of axons, despite clear interference with their continued extension, may indicate that growth was initiated before LIS1 levels had become severely reduced. These considerations suggest that LIS1 is not required for maintenance of processes once they have formed.

How LIS1 and dynein function to control process dynamics has been the subject of recent investigation. Inhibition of cytoplasmic dynein function using dynamitin was reported to induce myosin-mediated neurite retraction (Ahmad et al., 2000). We have more recently found that both LIS1 and dynein become concentrated at sites of nascent process formation at the leading edge of chick sympathetic and dorsal root ganglia growth cones in response to laminin and that they persist at the tips of rapidly growing processes (unpublished data). Acute interference with either LIS1 or dynein by antibody injection eliminated growth cone remodeling. We suspect that related effects occur in the axons of SVZ cells that were transfected with

LIS1 shRNA. Why the extension of axons would be more sensitive to reduced LIS1 expression than the growth of migratory processes (see previous section) is uncertain. However, our results suggest that elongation of the two types of process is controlled by substantially different mechanisms.

The function of early appearing axonal processes characterized in this study is not well established, and the effects that we observed on their extension had not been anticipated from prior studies. Use of retrograde tracing has shown connectivity of migrating neurons in the fetal monkey cerebrum to the opposite cerebral hemisphere (Schwartz and Goldman-Rakic, 1991). The processes that we observed (Fig. 7) exhibited organized and directed growth toward the midline of the cerebrum, strongly suggesting that they correspond to those involved in connectivity to other brain regions. The truncated axons that result from reduced LIS1 expression seem unlikely to be capable of reaching their targets. Our results, therefore, raise the novel possibility that similar, albeit less pronounced, effects may be involved in lissencephaly. Previous studies in hippocampus of LIS1 heterozygous mice and fruit flies showed stunted dendritic branches and abnormal synaptic transmission (Fleck et al., 2000; Liu et al., 2000). The effects on axon outgrowth that are identified in this study could well result in connectivity defects (Ross, 2002). These, in turn, may have severe consequences for brain function and could contribute to the loss of higher brain function, the frequency of epilepsy, cerebral palsy, and seizures that are characteristic of classical lissencephaly, and dramatically decreased life span.

Materials and methods

RNAi and dominant negative constructs

For RNAi, shRNA constructs based on the pRNAT-U6.1/Neo vector (GenScript), which expresses a GFP marker along with a sh siRNA, and Cy3-labeled synthetic siRNA oligonucleotides (Dharmacon) were used. Targeting sequences in the shRNA (pRNAT-LIS1; 5′-GAGAUGAACUAAAUCGAGCUA-3′) and siRNA oligonucleotide duplex (Cy3–5′-GAACAAGCGAUGCAUGAAGdTdT-3′) were chosen from a portion of the LIS1-coding region, where the sequence is identical among humans, African green monkeys, cows, rats, and mice. A triple mutated sequence in the pRNAT-LIS1 construct (pRNAT-LIS1-3mt; 5′-GACAUCAAGUAAAUCGAGCUA-3′) and a scrambled sequence of the same GC contents (Cy3–5′-AUUGUAUGCGAUCGCAGACdTdT-3′) are used as controls. No other related sequences were found in other sequences in the genome of these species. To construct dominant negative LIS1-GFP fusions, full-length African green monkey LIS1 (Faulkner et al., 2000) and a sequence encoding the first 87 NH_2-terminal aa (Tai et al., 2002) were made by PCR (primers: forward, 5′-GGAAGATCTCCAGGAATTCTGCTGTCCC-3′; LIS1 reverse, 5′-TAACCGCGGCCGCTCAACG-3′; and LIS1N reverse, 5′-TAACCGCGGCCGCTACTGACC-3′) using PfuTurbo DNA polymerase (Stratagene). The PCR products were then restriction enzyme digested and shuttled into BglII and SacII sites of pEGFP-C1 (CLONTECH Laboratories, Inc.).

In vitro RNAi assay

For transient transfection with pRNAT constructs, cells were plated on six-well dishes to 70–80% confluency and were transfected using LipofectAMINE 2000 (Invitrogen). For transient transfection with siRNA oligonucleotides, cells were plated on six-well dishes to 40–50% confluency and were transfected using OligofectAMINE (Invitrogen). Cells were lysed 45–48 h after transfection in 50 mM Tris-HCl, pH 8.0, 150 mM NaCl, 1% NP-40, and 1 mM EGTA with protease inhibitor cocktail for mammalian tissues (Sigma-Aldrich). pAb anti-LIS1 (Santa Cruz Biotechnology, Inc.) and mAb antitubulin (Sigma-Aldrich) were used for Western blotting.

In utero electroporation

Plasmids or oligonucleotides were transfected using intraventricular injection followed by in utero electroporation (Saito and Nakatsuji, 2001; Tabata and Nakajima, 2001). In brief, pregnant Sprague Dawley rats (Taconic) were used, and 1–2 μl cDNA (1–5 μg/μl) or 1 μg/μl siRNA were injected into the ventricle of embryonic brains at E16. A pair of copper alloy oval plates that were attached to the electroporation generator (Harvard Apparatus) transmitted five electric pulses at 50 V for 50 ms at 1-s intervals through the uterine wall. Animals were maintained according to protocols approved by the Institutional Animal Care and Use Committee at Columbia University.

Immunocytochemistry

Rat embryos were perfused transcardially with ice-chilled saline followed by 4% PFA (EMS) in 0.1 M PBS, pH7.4. Brains were postfixed in PFA overnight and sectioned on a Vibrotome (Ted Pella). Slices were blocked at RT for 1 h with 10% serum, 0.1% Triton X-100, and 0.2% gelatin in PBS. Primary antibodies were applied overnight at the following concentrations: anti-LIS1, 1:200 (gift from M. Mizuguchi, University of Tokyo, Tokyo, Japan; Mizuguchi et al., 1995); anti-TuJ1, 1:40 (Babco); antinestin, 1:200 (Chemicon), antivimentin, 1:40 (CBL); 4A4, 1:1,000 (MBL International Corporation); and anti-Ki67, 1:200 (Chemicon). Sections were then washed with PBS and incubated in Cy5-conjugated secondary antibodies (1:200; Jackson ImmunoResearch Laboratories).

Confocal microscopy

Sections were imaged on an inverted laser-scanning confocal microscope (FluoView 300; Olympus) with a 40× NA 0.8 water immersion objective (Olympus). Excitation/emission wavelengths were 488/515 nm (GFP), 568/590 nm (DsRed), and 633/690 (Cy5). Z-series images were collected at 2–3-μm steps in FluoView, and a projection of each stack was used for producing figures. Images were contrast enhanced, assembled into montages, and false color was applied using Photoshop (Adobe). In each brain slice, 100–500 cells could be found positive to GFP when electroporated with the constructs used. When Cy3-labeled synthetic siRNA oligonucleotides were used, 30–80 siRNA-positive cells per slice could be detected. These cells were all counted for statistic analysis (Table S1). In experiments that involved colabeling or cell/process counting, images from individual optical sections were carefully examined.

Live cell imaging

Coronal slices were prepared 24–48 h after electroporation. Slices were placed on Millicell-CM inserts (Millipore) in culture medium containing 25% Hanks balanced salt solution, 47% basal MEM, 25% normal horse serum, 1× penicillin/streptomycin/glutamine (GIBCO BRL), and 0.66% glucose and were incubated at 37°C in 5% CO_2. Multiple GFP-positive cells (Table S2) were imaged on an inverted microscope (model DMIRB; Leica) with a 40× NA 0.55 objective. Time-lapse images were captured by camera (CoolSNAP HQ; Roper Scientific) using MetaMorph software (Universal Imaging Corp.) at intervals of 10 or 15 min for 10–18 h. Epifluorescence images from several focal planes were deconvolved using AutoDeblur software (AutoQuant Imaging, Inc.) to produce sharp images.

Online supplemental material

Fig. S1 shows that neuronal migration occurs radially but also along curved radial glial fiber tracks. Fig. S2 shows that multipolar morphology is predominant in neural progenitor cells that were transfected with Cy3-LIS1 siRNA oligonucleotides or dominant negative LIS1 and dynamitin constructs. Fig. S3 shows that multipolar cells expressing LIS1 shRNA are positive for the neuronal marker TuJ1. Tables S1 and S2 summarize the number of embryos that were used and cells that were counted in this study. Videos S1–S10 demonstrate the behavior of neural progenitor cells at different stages and areas in live preparations of normal and LIS1 shRNA–transfected brains. Online supplemental material is available at http://www.jcb.org/cgi/content/full/jcb.200505166/DC1.

We would like to thank Joy Mirjahangir and Dr. Kathleen Bremner for extensive help during surgical procedures and Dr. Peter Canoll and Dr. Stephan Noctor for helpful comments and suggestions throughout the project.

This work was supported by National Institutes of Health (NIH) grant 40182, a grant from the March of Dimes Birth Defects Foundation to R.B. Vallee, and NIH grants NS21223 and NS35710 to A.R. Kriegstein.

Submitted: 26 May 2005
Accepted: 3 August 2005

References

Ahmad, F.J., J. Hughey, T. Wittmann, A. Hyman, M. Greaser, and P.W. Baas. 2000. Motor proteins regulate force interactions between microtubules and microfilaments in the axon. *Nat. Cell Biol.* 2:276–280.

Cahana, A., T. Escamez, R.S. Nowakowski, N.L. Hayes, M. Giacobini, A. von Holst, O. Shmueli, T. Sapir, S.K. McConnell, W. Wurst, et al. 2001. Targeted mutagenesis of Lis1 disrupts cortical development and LIS1 homodimerization. *Proc. Natl. Acad. Sci. USA.* 98:6429–6434.

Dobyns, W.B., and C.L. Truwit. 1995. Lissencephaly and other malformations of cortical development: 1995 update. *Neuropediatrics.* 26:132–147.

Dujardin, D.L., L.E. Barnhart, S.A. Stehman, E.R. Gomes, G.G. Gundersen, and R.B. Vallee. 2003. A role for cytoplasmic dynein and LIS1 in directed cell movement. *J. Cell Biol.* 163:1205–1211.

Echeverri, C.J., B.M. Paschal, K.T. Vaughan, and R.B. Vallee. 1996. Molecular characterization of the 50-kD subunit of dynactin reveals function for the complex in chromosome alignment and spindle organization during mitosis. *J. Cell Biol.* 132:617–633.

Efimov, V.P., and N.R. Morris. 2000. The LIS1-related NUDF protein of *Aspergillus nidulans* interacts with the coiled-coil domain of the NUDE/RO11 protein. *J. Cell Biol.* 150:681–688.

Etienne-Manneville, S., and A. Hall. 2001. Integrin-mediated activation of Cdc42 controls cell polarity in migrating astrocytes through PKCzeta. *Cell.* 106:489–498.

Faulkner, N.E., D.L. Dujardin, C.Y. Tai, K.T. Vaughan, C.B. O'Connell, Y. Wang, and R.B. Vallee. 2000. A role for the lissencephaly gene LIS1 in mitosis and cytoplasmic dynein function. *Nat. Cell Biol.* 2:784–791.

Feng, Y., and C.A. Walsh. 2004. Mitotic spindle regulation by Nde1 controls cerebral cortical size. *Neuron.* 44:279–293.

Fleck, M.W., S. Hirotsune, M.J. Gambello, E. Phillips-Tansey, G. Suares, R.F. Mervis, A. Wynshaw-Boris, and C.J. McBain. 2000. Hippocampal abnormalities and enhanced excitability in a murine model of human lissencephaly. *J. Neurosci.* 20:2439–2450.

Gambello, M.J., D.L. Darling, J. Yingling, T. Tanaka, J.G. Gleeson, and A. Wynshaw-Boris. 2003. Multiple dose-dependent effects of Lis1 on cerebral cortical development. *J. Neurosci.* 23:1719–1729.

Geiser, J.R., E.J. Schott, T.J. Kingsbury, N.B. Cole, L.J. Totis, G. Bhattacharyya, L. He, and M.A. Hoyt. 1997. *Saccharomyces cerevisiae* genes required in the absence of the CIN8-encoded spindle motor act in functionally diverse mitotic pathways. *Mol. Biol. Cell.* 8:1035–1050.

Gupta, A., K. Sanada, D.T. Miyamoto, S. Rovelstad, B. Nadarajah, A.L. Pearlman, J. Brunstrom, and L.H. Tsai. 2003. Layering defect in p35 deficiency is linked to improper neuronal-glial interaction in radial migration. *Nat. Neurosci.* 6:1284–1291.

Hattori, M., H. Adachi, M. Tsujimoto, H. Arai, and K. Inoue. 1994. Miller-Dieker lissencephaly gene encodes a subunit of brain platelet-activating factor acetylhydrolase. *Nature.* 370:216–218 (corrected).

Haubensak, W., A. Attardo, W. Denk, and W.B. Huttner. 2004. Neurons arise in the basal neuroepithelium of the early mammalian telencephalon: a major site of neurogenesis. *Proc. Natl. Acad. Sci. USA.* 101:3196–3201.

Hirotsune, S., M.W. Fleck, M.J. Gambello, G.J. Bix, A. Chen, G.D. Clark, D.H. Ledbetter, C.J. McBain, and A. Wynshaw-Boris. 1998. Graded reduction of Pafah1b1 (Lis1) activity results in neuronal migration defects and early embryonic lethality. *Nat. Genet.* 19:333–339.

Kholmanskikh, S.S., J.S. Dobrin, A. Wynshaw-Boris, P.C. Letourneau, and M.E. Ross. 2003. Disregulated RhoGTPases and actin cytoskeleton contribute to the migration defect in Lis1-deficient neurons. *J. Neurosci.* 23:8673–8681.

Kitagawa, M., M. Umezu, J. Aoki, H. Koizumi, H. Arai, and K. Inoue. 2000. Direct association of LIS1, the lissencephaly gene product, with a mammalian homologue of a fungal nuclear distribution protein, rNUDE. *FEBS Lett.* 479:57–62.

Koizumi, H., N. Yamaguchi, M. Hattori, T.O. Ishikawa, J. Aoki, M.M. Taketo, K. Inoue, and H. Arai. 2003. Targeted disruption of intracellular type I platelet activating factor-acetylhydrolase catalytic subunits causes severe impairment in spermatogenesis. *J. Biol. Chem.* 278:12489–12494.

Liu, Z., R. Steward, and L. Luo. 2000. *Drosophila* Lis1 is required for neuroblast proliferation, dendritic elaboration and axonal transport. *Nat. Cell Biol.* 2:776–783.

Lo Nigro, C., C.S. Chong, A.C. Smith, W.B. Dobyns, R. Carrozzo, and D.H. Ledbetter. 1997. Point mutations and an intragenic deletion in LIS1, the lissencephaly causative gene in isolated lissencephaly sequence and Miller-Dieker syndrome. *Hum. Mol. Genet.* 6:157–164.

LoTurco, J. 2004. Doublecortin and a tale of two serines. *Neuron.* 41:175–177.

Malatesta, P., E. Hartfuss, and M. Gotz. 2000. Isolation of radial glial cells by fluorescent-activated cell sorting reveals a neuronal lineage. *Development.* 127:5253–5263.

Misson, J.P., C.P. Austin, T. Takahashi, C.L. Cepko, and V.S. Caviness Jr. 1991. The alignment of migrating neural cells in relation to the murine neopallial radial glial fiber system. *Cereb. Cortex.* 1:221–229.

Miyata, T., A. Kawaguchi, H. Okano, and M. Ogawa. 2001. Asymmetric inheritance of radial glial fibers by cortical neurons. *Neuron.* 31:727–741.

Mizuguchi, M., S. Takashima, A. Kakita, M. Yamada, and K. Ikeda. 1995. Lissencephaly gene product. Localization in the central nervous system and loss of immunoreactivity in Miller-Dieker syndrome. *Am. J. Pathol.* 147:1142–1151.

Morris, S.M., U. Albrecht, O. Reiner, G. Eichele, and L.Y. Yu-Lee. 1998. The lissencephaly gene product Lis1, a protein involved in neuronal migration, interacts with a nuclear movement protein, NudC. *Curr. Biol.* 8:603–606.

Nadarajah, B., J.E. Brunstrom, J. Grutzendler, R.O. Wong, and A.L. Pearlman. 2001. Two modes of radial migration in early development of the cerebral cortex. *Nat. Neurosci.* 4:143–150.

Niethammer, M., D.S. Smith, R. Ayala, J. Peng, J. Ko, M.S. Lee, M. Morabito, and L.H. Tsai. 2000. NUDEL is a novel Cdk5 substrate that associates with LIS1 and cytoplasmic dynein. *Neuron.* 28:697–711.

Noctor, S.C., A.C. Flint, T.A. Weissman, R.S. Dammerman, and A.R. Kriegstein. 2001. Neurons derived from radial glial cells establish radial units in neocortex. *Nature.* 409:714–720.

Noctor, S.C., V. Martinez-Cerdeno, L. Ivic, and A.R. Kriegstein. 2004. Cortical neurons arise in symmetric and asymmetric division zones and migrate through specific phases. *Nat. Neurosci.* 7:136–144.

Palazzo, A.F., H.L. Joseph, Y.J. Chen, D.L. Dujardin, A.S. Alberts, K.K. Pfister, R.B. Vallee, and G.G. Gundersen. 2001. Cdc42, dynein, and dynactin regulate MTOC reorientation independent of Rho-regulated microtubule stabilization. *Curr. Biol.* 11:1536–1541.

Rakic, P., L.J. Stensas, E. Sayre, and R.L. Sidman. 1974. Computer-aided three-dimensional reconstruction and quantitative analysis of cells from serial electron microscopic montages of foetal monkey brain. *Nature.* 250:31–34.

Reiner, O., R. Carrozzo, Y. Shen, M. Wehnert, F. Faustinella, W.B. Dobyns, C.T. Caskey, and D.H. Ledbetter. 1993. Isolation of a Miller-Dieker lissencephaly gene containing G protein beta-subunit-like repeats. *Nature.* 364:717–721.

Ross, M.E. 2002. Brain malformations, epilepsy, and infantile spasms. *Int. Rev. Neurobiol.* 49:333–352.

Saito, T., and N. Nakatsuji. 2001. Efficient gene transfer into the embryonic mouse brain using in vivo electroporation. *Dev. Biol.* 240:237–246.

Sasaki, S., A. Shionoya, M. Ishida, M.J. Gambello, J. Yingling, A. Wynshaw-Boris, and S. Hirotsune. 2000. A LIS1/NUDEL/cytoplasmic dynein heavy chain complex in the developing and adult nervous system. *Neuron.* 28:681–696.

Schwartz, M.L., and P.S. Goldman-Rakic. 1991. Prenatal specification of callosal connections in rhesus monkey. *J. Comp. Neurol.* 307:144–162.

Shu, T., R. Ayala, M.D. Nguyen, Z. Xie, J.G. Gleeson, and L.H. Tsai. 2004. Ndel1 operates in a common pathway with LIS1 and cytoplasmic dynein to regulate cortical neuronal positioning. *Neuron.* 44:263–277.

Smith, D.S., M. Niethammer, R. Ayala, Y. Zhou, M.J. Gambello, A. Wynshaw-Boris, and L.H. Tsai. 2000. Regulation of cytoplasmic dynein behaviour and microtubule organization by mammalian Lis1. *Nat. Cell Biol.* 2:767–775.

Solecki, D.J., L. Model, J. Gaetz, T.M. Kapoor, and M.E. Hatten. 2004. Par6alpha signaling controls glial-guided neuronal migration. *Nat. Neurosci.* 7:1195–1203.

Tabata, H., and K. Nakajima. 2001. Efficient in utero gene transfer system to the developing mouse brain using electroporation: visualization of neuronal migration in the developing cortex. *Neuroscience.* 103:865–872.

Tabata, H., and K. Nakajima. 2003. Multipolar migration: the third mode of radial neuronal migration in the developing cerebral cortex. *J. Neurosci.* 23:9996–10001.

Tai, C.Y., D.L. Dujardin, N.E. Faulkner, and R.B. Vallee. 2002. Role of dynein, dynactin, and CLIP-170 interactions in LIS1 kinetochore function. *J. Cell Biol.* 156:959–968.

Tanaka, T., F.F. Serneo, C. Higgins, M.J. Gambello, A. Wynshaw-Boris, and J.G. Gleeson. 2004. Lis1 and doublecortin function with dynein to mediate coupling of the nucleus to the centrosome in neuronal migration. *J. Cell Biol.* 165:709–721.

Xiang, X., A.H. Osmani, S.A. Osmani, M. Xin, and N.R. Morris. 1995. NudF, a nuclear migration gene in *Aspergillus nidulans*, is similar to the human LIS-1 gene required for neuronal migration. *Mol. Biol. Cell.* 6:297–310.

Yan, W., A.H. Assadi, A. Wynshaw-Boris, G. Eichele, M.M. Matzuk, and G.D. Clark. 2003. Previously uncharacterized roles of platelet-activating factor acetylhydrolase 1b complex in mouse spermatogenesis. *Proc. Natl. Acad. Sci. USA.* 100:7189–7194.